

# Light and Electron-Microscopic Studies on the Paraepiglottic Tonsil of the Buffalo (*Bubalus bubalis*)

Ibrahim Alhaji Girgiri and Pawan Kumar\*

*Department of Veterinary Anatomy, College of Veterinary Sciences, Lala Lajpat Rai University of Veterinary and Animal Sciences, Hisar-125 004, India*

**Abstract:** The paraepiglottic tonsil present on either side of the base of the epiglottis constitutes a small portion of the mucosa-associated lymphoid tissue. The present study was conducted on the paraepiglottic tonsils of 12 adult buffaloes of the local mixed breed to explore its basic histomorphological, histochemical, and ultrastructural characteristics and to compare with other tonsils of the oral region to ascribe immunological function. The tonsil mucosa was lined by partly stratified squamous keratinised epithelium towards the outer surface and a stratified squamous non-keratinised epithelium towards the shallow crypts. The non-keratinised epithelium modified into reticular type due to infiltration of underlying lymphoid tissue was characterised by the predominance of the lymphoid cells, interrupting basement membrane and indistinct strata. The reticular epithelium at places presented a spongy appearance. The loose irregular connective tissue of propria-submucosa was mainly comprised of glandular and lymphoid tissue. The lymphoid tissue was mainly in the form of isolated lymphocytes, diffuse aggregations, and lymphoid follicles. The inter-follicular areas showed the presence of high endothelial venules. The sero-mucous type of glandular acini presented a strong reaction for glycogen, acidic mucosubstances, weakly sulfated mucosubstances, mucin, and the presence of more than 4% cysteine in their secretions. The tonsils under scanning electron microscopy presented an undulating appearance due to the presence of crest and folds. Higher magnification revealed squamous cells having various patterns and arrangements of microplacae. Small pits visualised on the mucosal surface represented openings of the glandular ducts. The cells towards the lumen of some glandular ducts appeared whorl-like where typical microplacae were absent. The transmission electron microscopy of different strata of different types of epithelia showed varying cell organelles, especially the mitochondria, endoplasmic reticulum, Golgi apparatus, and few filaments. The structural features of the tonsil were similar to those of other oral tonsils and suggested their immunological role, which might be of importance to local immunity.

**Keywords:** Buffalo, High endothelial venule, Microplacae, Paraepiglottic tonsil, Reticular epithelium.

## INTRODUCTION

Tonsils are major components of mucosa-associated lymphoid tissue (MALT) comprised of special lymphoid aggregates integrated into the different parts of pharyngeal mucosa of the upper aero-digestive tract [1]. Their immune specialised cellular architecture, including reticular crypt epithelium, germinal centres in B-cell follicles, and extra-follicular areas rich in T-cells, resembles that of lymph nodes, although the absence of afferent lymphatics implies a reliance on direct interaction with environmental antigens [2]. Tonsils are involved in innate, cellular, and humoral immunity, and continuous surveillance against foreign antigens taken up during feeding and breathing [3] and act as inductive sites to stimulate cognate naive T and B lymphocytes [4]. The strategic location of the tonsils determines their important role as secondary lymphoid tissue in the immunological response to antigens [5]. Six types of tonsils described in domestic mammals vary in terms of their existence and locations [6]. The detailed anatomical structure of the tonsil of the soft palate [7, 8], palatine tonsil [9, 10], nasopharyngeal

tonsil [11], lingual tonsil [12-14], and the tubal tonsil [15] has been described in the buffaloes. The paraepiglottic tonsil is absent in the horse, ox, and dog, whereas inconsistent in the goat [16]. The microscopic structure of paraepiglottic lymphoid tissue has been described in young cattle [17], sheep [18], and pigs [19]. The perusal of literature revealed a lack of study on the architecture of the paraepiglottic tonsil in the buffaloes. Hence, the present study was initiated to describe the structural characteristics of the tonsil and to compare it with other tonsils that could offer better insight to ascribe its role in the induction of immune responses in the buffalo.

## MATERIALS AND METHODS

The paraepiglottic tonsils located on either side at the base of the epiglottis were collected from twelve adult buffaloes (5-6 years old) of local mixed breed following their sacrifice by captive bolt stunning gun method at the slaughterhouse, Ghazipur, New Delhi. Approval of the Institutional Animal Ethical Committee was not required as the tissues were collected from the slaughterhouse after the death of the animals.

## Histomorphology and Histochemistry

The tonsils from six animals fixed in 10% neutral buffered formalin solution for 48 hours at room

\*Address correspondence to this author at the Department of Veterinary Anatomy, College of Veterinary Sciences, Lala Lajpat Rai University of Veterinary and Animal Sciences, Hisar-125 004, India; Tel: +919466402637; E-mail: pkumar@luvas.edu.in, pawanrajoria2000@rediffmail.com

temperature were processed by paraffin technique. The paraffin sections of 5-6  $\mu\text{m}$  were stained with routine Harris' hematoxylin and eosin stain, Gomori's method for reticulum, Weigert's method for elastic fibres, [20]; Crossman's trichrome stain for collagen fibres [21], McManus' method for glycogen (PAS), Alcian blue method for muco-substances (pH 2.5), PAS-Alcian blue method for acidic and neutral mucosubstances (pH 2.5), Meyer's mucicarmine method for mucin, the colloidal iron method for acid mucopolysaccharides [20]; and performic acid-Alcian blue method for proteins [22].

### Scanning Electron-Microscopy (SEM)

Fresh tissue samples of the tonsils collected from the other 6 heads were thoroughly washed with chilled 0.1M phosphate buffer (pH 7.4) and fixed in 2% glutaraldehyde solution for 6-8 hours at 4°C. The tissues were rewashed twice with 0.1M phosphate buffer, and the rest of the procedure was carried out at EM Lab., AIRF, JNU, and AIIMS, New Delhi. The tissues were dehydrated using ascending grades of alcohol, critical point dried, mounted on stubs and sputter-coated with gold. The processed tissues were viewed using a scanning electron microscope (Zeiss EVO-40, New York, USA) at EM Labs., New Delhi.

### Transmission Electron-Microscopy (TEM)

The small pieces of paraepiglottic tonsils were primarily fixed in 2.5% glutaraldehyde solution for 6-8 hours at 4°C and post-fixed in 2% osmium tetroxide for 1 hour at 4°C. The epoxy resin blocks were prepared, and thin sections of 1  $\mu\text{m}$  were stained with toluidine blue to select the most appropriate area of the tissue. The ultrathin sections (50-70 nm) taken on copper grids were stained with 3% uranyl acetate for 10-15mins followed by 0.4% lead citrate for 5-10mins. The grids were viewed in a transmission electron microscope (Technai G2, SEI Co., Netherland) to record the observations and photographs.

## RESULTS

### Histomorphology and Histochemistry

The paraepiglottic tonsil towards its outer surface was lined by stratified squamous partly keratinised (Figure 1) to the non-keratinised type of epithelium. The epithelium was comprised of a varying number of rows in different strata (Figure 2). The stratum basale was comprised of a single row of cells that contained round to oval nuclei toward the basement membrane.



**Figure 1:** Photomicrograph of the paraepiglottic tonsil of buffalo showing stratified squamous keratinised epithelium (E), interpapillary pegs (arrow), and loose irregular connective tissue (T) of the lamina propria having duct (D), and lymphoid tissue (L). H & E  $\times$  100; (bar 200  $\mu\text{m}$ ).

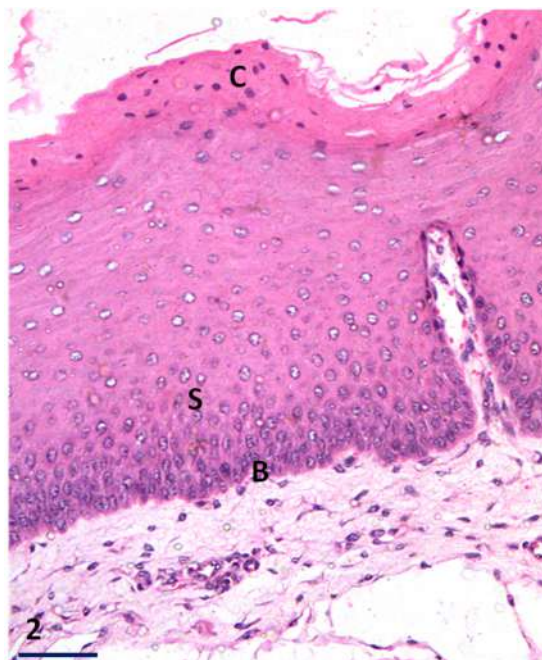


**Figure 2:** Photomicrograph of the paraepiglottic tonsil of buffalo showing stratum basale (B), stratum spinosum (S), stratum granulosum and stratum corneum (C) of stratified squamous keratinised epithelium. H & E  $\times$  200; (bar 100  $\mu\text{m}$ ).

The basophilic nuclei contained smaller clumps of chromatin throughout the nucleoplasm. Some of the nuclei were comparatively less basophilic and presented some vacuolated appearance due to

condensation of chromatin towards the outer nuclear membrane. The nuclei generally contained one centric/eccentric nucleolus. The eosinophilic cytoplasm of these cells was finely granular. At some places, a few lymphocytes infiltrated in between these cells.

The stratum spinosum was comprised of a varying number of rows of round to oval nuclei. The deeper cells had histological features similar to those of the basal cells. The rest of the nuclei were larger in size, fewer in number, comparatively less basophilic and generally contained 1-2 centric/eccentric nucleoli. The cytoplasm of these cells was finely granular and eosinophilic in nature.

The stratum granulosum layer also showed a varying number of rows of nuclei which were very widely placed and lesser in number. These cells had eosinophilic cytoplasm and less basophilic nuclei. The stratum corneum also showed a varying number of rows of nuclei which were further reduced in size as compared to those of stratum granulosum. These nuclei were deeply basophilic because of a dense arrangement of chromatin material, and thus the nucleoli were not distinctly visible in the majority of these nuclei. Some of the nuclei were also observed very close to the surface of the epithelium, which showed degenerative changes. The cytoplasm of these cells was strongly eosinophilic and finely granular in nature (Figure 2). The basal surface of the epithelium showed the presence of interpapillary pegs (Figure 1), which were comparatively broader and of irregular shapes, whereas the free surface presented an undulating surface.

The surface epithelium lining the small crypts or depressions was modified into a stratified squamous non-keratinised type which was generally associated with underlying lymphoid tissue (Figure 3). The non-keratinised epithelium had strata basale, spinosum and superficiale. The crypt surface was slightly uneven, whereas the basal surface was almost uniform. The histological structure of cells of stratum basale and stratum spinosum had characteristics similar to described in the keratinised epithelium. However, the latter lacked a prickly appearance (Figure 3). The cells of the stratum superficiale were also varying in number and rows at different levels of extents of the epithelium. The nuclei of more superficially placed cells were more basophilic and presented degenerative changes (Figure 3). The eosinophilic cytoplasm of these cells was also finely granular.

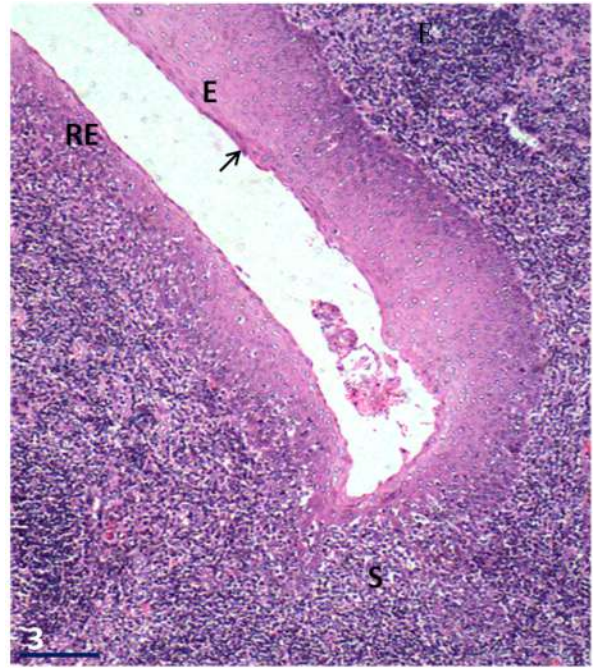


**Figure 3:** Photomicrograph of the paraepiglottic tonsil of buffalo showing a modification of stratified squamous non-keratinised epithelium (E) into reticular epithelium (RE) towards the depression or shallow crypt. The deeply basophilic nuclei (arrow) of the superficial cells show degenerative changes. Note the spongy appearance of the epithelium (S) due to heavy infiltration of the lymphoid tissue. H & E  $\times$  100; (bar 200  $\mu$ m).

At some places, the stratified squamous non-keratinised epithelium further showed modification in the form of reticular epithelium, where the underlying lymphoid tissue penetrated the epithelium (Figure 3). The reticular epithelium present in the form of small irregular patches lacked distinct strata. Generally, there was a predominance of the lymphoid cells than epithelial cells. At these places, the basement membrane was interrupted, and the lymphoid cells also reached up to the surface of the epithelium. Only a few epithelial cells with indistinct strata were interspersed with those of the lymphoid cells (Figure 3). The reticular epithelium at a few places presented a spongy appearance due to the lack of distinct strata and continuity of the cells, and it was difficult to discern the epithelial and the lymphoid cells because of the predominance of the infiltration of the lymphoid cells (Figure 3).

The propria-submucosa had loose irregular connective tissue (Figure 1) being comprised of collagen, reticular and elastic fibres, fine blood capillaries, blood vessels of different sizes, lymphoid tissue, glandular tissue and a few nerve bundles. Collagen bundles surrounded the glandular acini, lymphoid tissue, and inter-glandular region. The

reticular fibres formed the basement membrane, which was interrupted in the region of the reticular epithelium. Their concentration increased in the glandular, lymphoid and parafollicular areas. The elastic fibres were present in the subepithelial portion, interglandular region, ventral to the lymphoid aggregations and in the tunica intima of blood vessels.

The lymphoid tissue was distributed in the form of isolated lymphocytes that penetrated the epithelium, especially the reticular epithelium, diffuse aggregations and lymphoid follicles. The follicles had a lighter stained germinal centre and darkly stained corona towards the periphery (Figure 4). The follicles were arranged adjacent to each other with inter-follicular areas; however, these were stacked one upon another towards the depression or small crypt region. The follicles were comprised of lymphocytes of different sizes, a few plasma cells, and macrophages. High endothelial venules, fine blood capillaries, macrophages, and plasma cells were localised towards the periphery of the lymphoid follicles (Figure 5).

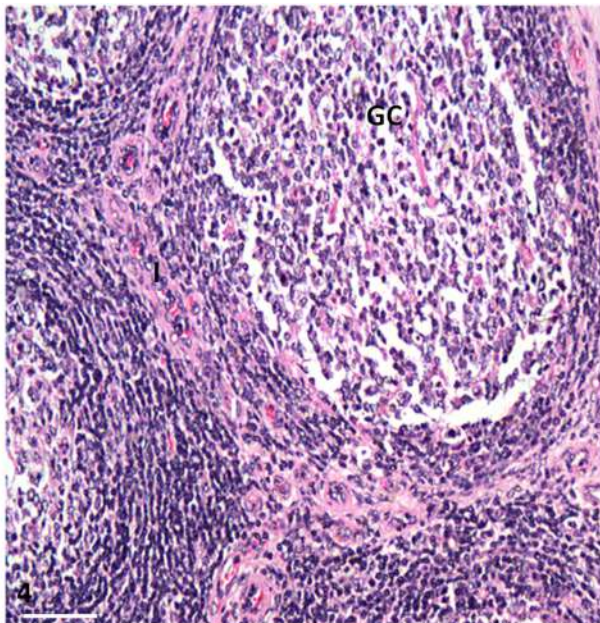


**Figure 4:** Photomicrograph of the paraepiglottic tonsil of buffalo showing germinal centre (GC), parafollicular (P) and inter-follicular area (I). H & E  $\times$  100; (bar 200  $\mu$ m).

The sero-mucous glandular acini present in small clusters were separated from each other by fine collagen, reticular and elastic fibres. The cytoplasm of mucous acini was slightly eosinophilic, finely granular and presented a vacuolated appearance. Only a few serous acini present in between the mucous type had comparatively more eosinophilic cytoplasm. The mucous acini were strongly positive by McManus' PAS

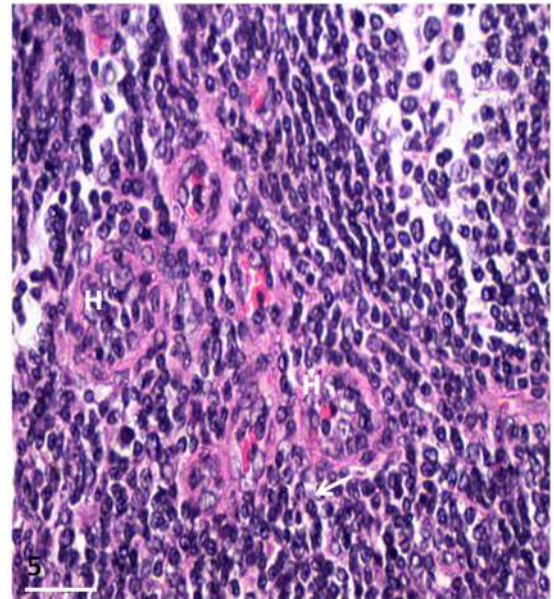


**Figure 5:** Photomicrograph of the inter-follicular area of paraepiglottic tonsil at higher magnification showing high endothelial venules (H) and plasma cells (arrow). H & E  $\times$  400; (bar 50  $\mu$ m).

method, indicating the presence of glycogen (Figure 6). These acini showed the presence of acidic and absence of neutral mucopolysaccharides by the PAS AB method (Figure 7). A similar pattern of acidic mucopolysaccharides was demonstrated by the colloidal iron method (Figure 8). A strong Alcianophilic reaction in the acini indicated the presence of weakly sulfated acidic mucosubstances, hyaluronic acid and sialomucins (Figure 9). Meyer's mucicarmin method

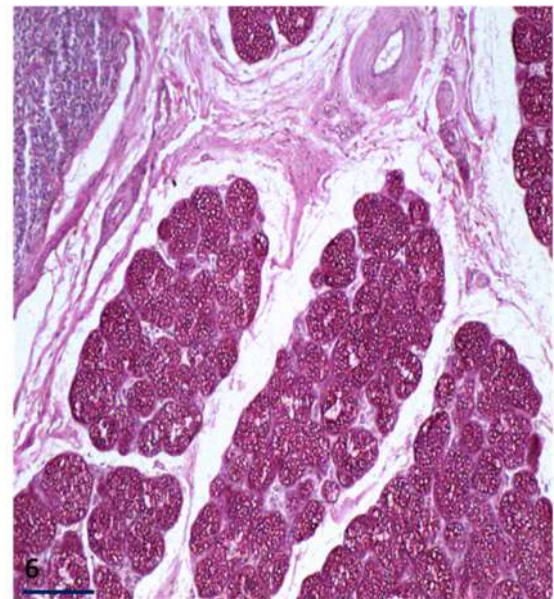


**Figure 6:** Photomicrograph of the paraepiglottic tonsil of buffalo showing strong PAS-positive reaction for glycogen (magenta colour) in the mucous glandular acini. McManus' PAS  $\times$  100; (bar 200  $\mu$ m).

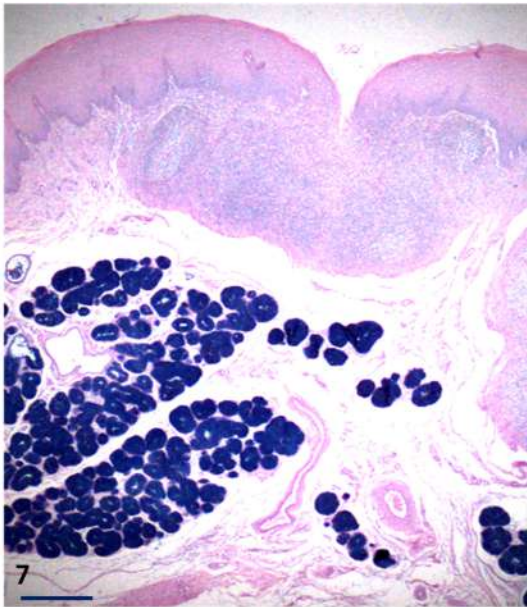


**Figure 7:** Photomicrograph of the paraepiglottic tonsil of buffalo showing strong PAS-positive activity of acidic mucopolysaccharides (blue colour) in the mucous glandular acini. PAS-AB  $\times 40$ ; (bar 450  $\mu\text{m}$ ).

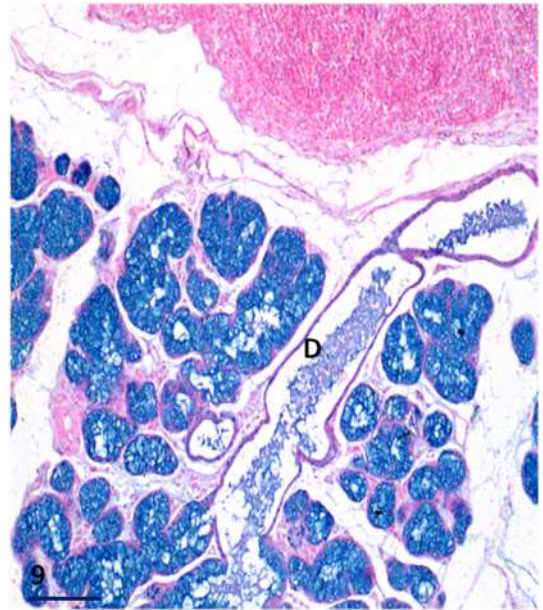


**Figure 9:** Photomicrograph of the paraepiglottic tonsil of buffalo showing the presence of weakly sulfated mucosubstances, sialomucin and hyaluronic acid (blue colour) in the mucous glandular acini and absence in the glandular duct (D). Alcian blue  $\times 100$ ; (bar 200  $\mu\text{m}$ ).

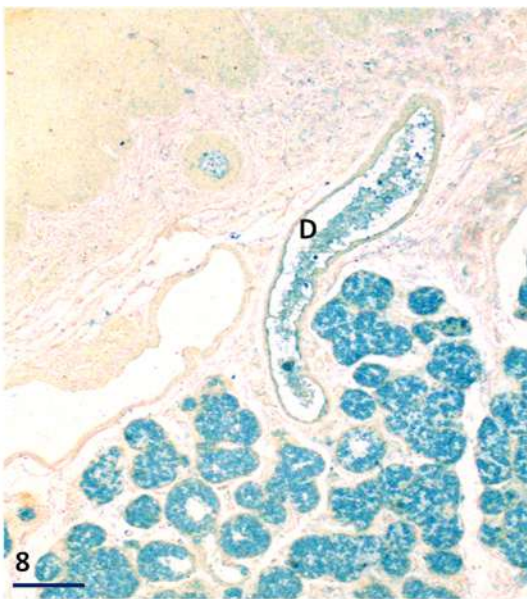


**Figure 8:** Photomicrograph of the paraepiglottic tonsil of buffalo showing the presence of the acidic mucopolysaccharides (green colour) in the mucous glandular acini and absence of reaction in the glandular duct (D). Colloidal iron  $\times 100$ ; (bar 200  $\mu\text{m}$ ).



**Figure 10:** Photomicrograph of the paraepiglottic tonsil of buffalo showing the distribution of mucin (rose-red colour) in the mucous glandular acini. Meyer's mucicarmin  $\times 100$ ; (bar 200  $\mu\text{m}$ ).

demonstrated the presence of mucin in the mucous glandular acini (Figure 10). The mucous acini showed a very strong reaction for performic acid-Alcian blue, indicating the presence of more than 4% cysteine (Figure 11). The intra and inter-glandular ducts were lined simple to the stratified cuboidal epithelium. These ducts coursed towards the surface of the epithelium.

**SEM**

The mucosal surface of the paraepiglottic tonsils, under a scanning electron microscope, showed several

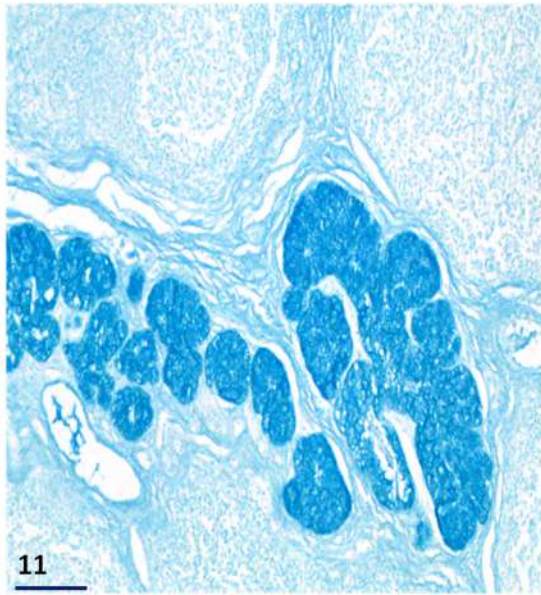


**Figure 11:** Photomicrograph of the paraepiglottic tonsil of buffalo showing more than 4% cysteine (blue colour) activity in mucous glandular acini. Performic acid Alcian blue  $\times 100$ ; (bar 200  $\mu\text{m}$ ).

folds separated by shallow grooves (Figure 12). The surface of these folds presented smaller crests and folds giving an undulating appearance (Figures 12 and 13) and was studded with squamous cells which were continuous with each other having microplacae (Figures 13 and 14). These cells at higher magnification showed varying patterns of the microplacae, including a honeycomb-like appearance (Figure 14). The adjacent

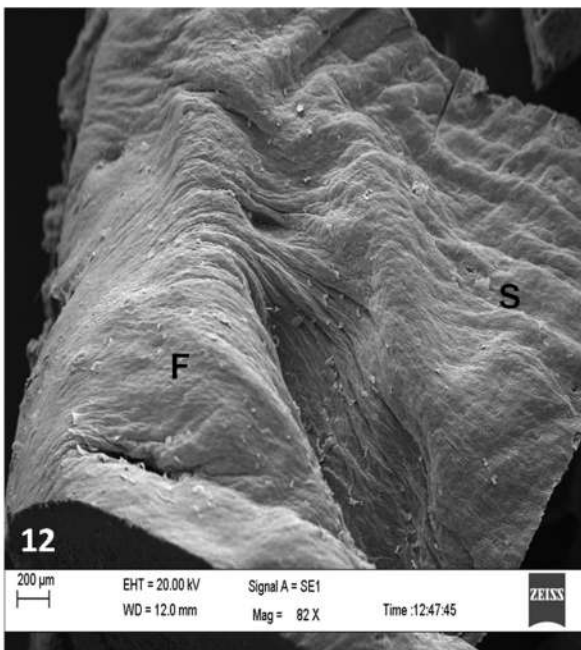


**Figure 12:** Scanning electron micrograph of the mucosal surface of the paraepiglottic tonsil of buffalo showing folds (F) separated by a shallow groove (S).  $\times 82$ ; (bar 200  $\mu\text{m}$ ).

squamous cells were separated by a thick arrangement.

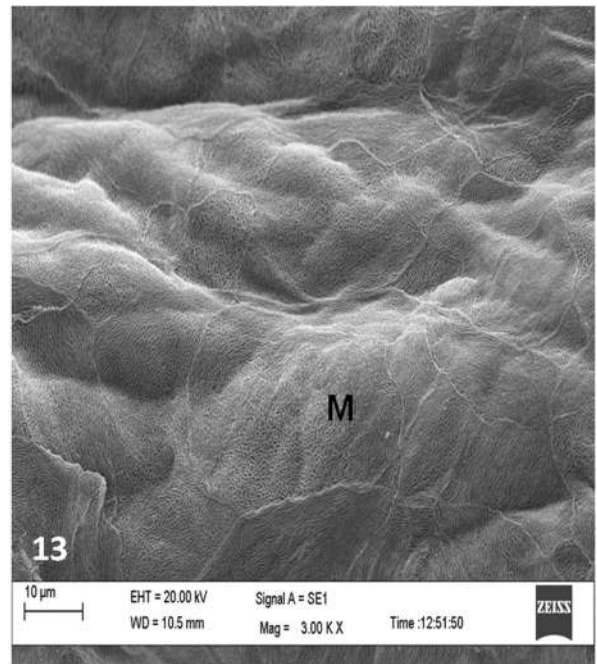


**Figure 13:** Scanning electron micrograph of the mucosal surface of the paraepiglottic tonsil of buffalo showing microplacae (M).  $\times 3000$ ; (bar 10  $\mu\text{m}$ ).

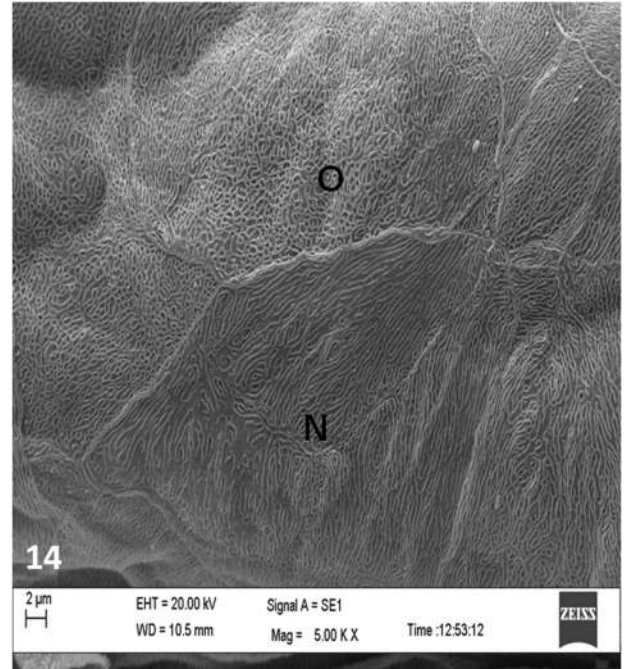


**Figure 14:** Scanning electron micrograph of the paraepiglottic tonsil of buffalo showing honeycomb (O) and human fingerprint (N) types of the microplacae.  $\times 5000$ ; (bar 2  $\mu\text{m}$ ).

This mucosal surface also showed few exfoliated cells. Small pits or holes observed on the surface



**Figure 15:** Scanning electron micrograph of the mucosal surface of the paraepiglottic tonsil of buffalo showing irregularly placed pits or holes (P). × 111; (bar 200 μm).

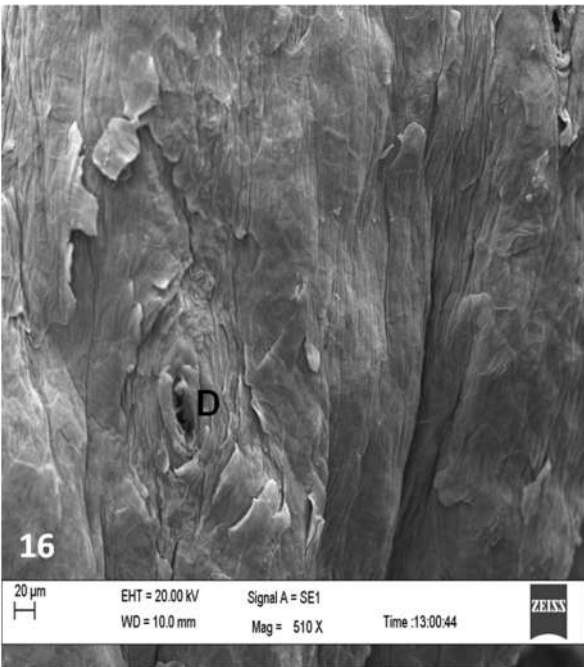


**Figure 16:** Scanning electron micrograph of the mucosal surface of the paraepiglottic tonsil of buffalo showing the opening of the glandular duct (D). × 510; (bar 20 μm).

represented the openings of the glandular ducts (Figures 15-18). These openings were obliterated due to the secretions of the glands, desquamated cells and the cells lining the lumen of the ducts (Figures 16 and 17). The lumen surface was surrounded by a whorl-like arrangement of the cells having small microvilli like arrangement, and the microplacae were absent (Figure

18). It was interesting to note that the surface of the tonsil just adjacent to the opening of the ducts had a typical arrangement of the microplacae (Figure 19).

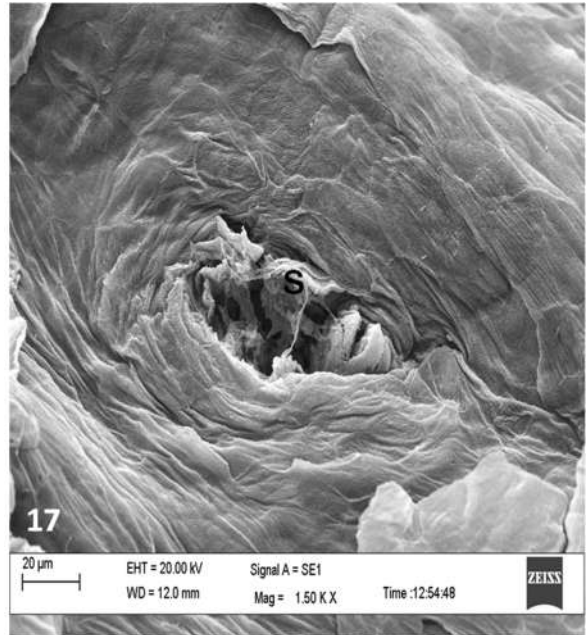


**Figure 17:** Scanning electron micrograph of glandular duct opening showing its obliteration by secretions or desquamating cells (S). × 1500; (bar 20 μm).



**Figure 18:** Scanning electron micrograph of the lumen of the glandular duct showing the whorl-like arrangement of the cells. × 2040; (bar 20 μm).

#### TEM

The paraepiglottic tonsils were lined by stratified squamous keratinised epithelium, which modified into

the reticular epithelium towards the depressions because of the infiltration of lymphoid cells from the underlying propria-submucosa.

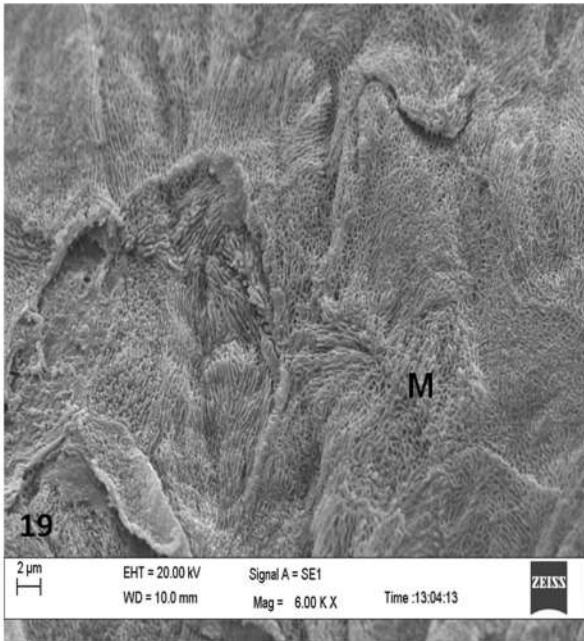


**Figure 19:** Scanning electron micrograph at higher magnification showing a typical arrangement of microvilli just adjacent to the surface of the duct (M).  $\times 6000$ ; (bar  $2 \mu\text{m}$ ).

The stratum basale had a single row of high cuboidal to columnar cells with vertically oriented nuclei (Figure 20). Moreover, these nuclei were less electron-dense and showed chromatin material irregularly arranged into smaller clumps throughout the nucleoplasm. These nuclei contained one to two nucleoli that were centric/eccentric in position. The outer surface of the nuclei was irregular and undulating, and some of these presented nuclear indentations. The cytoplasm had the distribution of varying cell organelles, especially the mitochondria, endoplasmic reticulum, Golgi apparatus and few filaments. The adjacent cells of the stratum basale were joined by desmosomes, and the intercellular spaces showed the presence of the interdigitating villi of varying shapes and sizes. Between the epithelial cells at different places, few lymphoid cells were seen, especially the lymphocytes (Figures 20 and 21).

The stratum spinosum had different rows of cells, and their nuclei were oriented in different directions. These nuclei were also electron-lucent, showing a small amount of electron-dense chromatin towards the outer nuclear membrane, and the nuclei generally contained one nucleolus, which was centric/eccentric in position. The distribution of the cell organelles in the

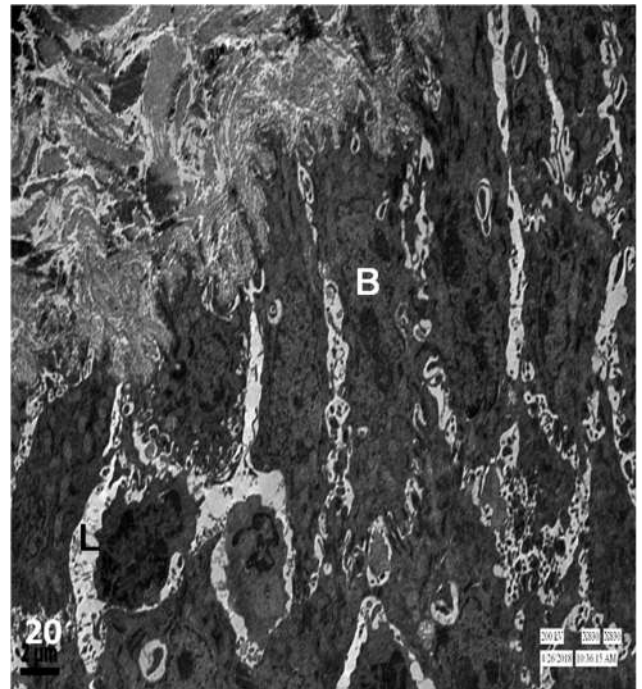


**Figure 20:** Transmission electron micrograph of the paraepiglottic tonsil of buffalo showing stratum basale (B) of keratinised epithelium infiltrated by isolated lymphocyte (L).  $\times 830$ ; (bar  $2 \mu\text{m}$ ).

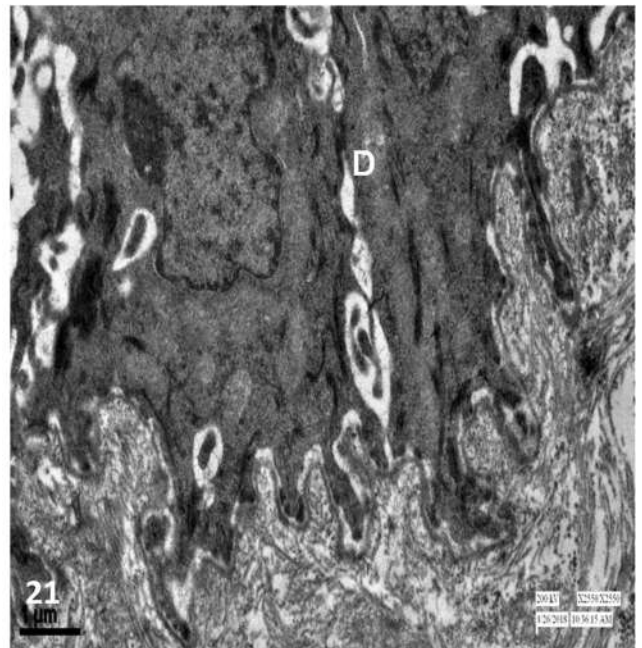


**Figure 21:** Transmission electron micrograph of the stratum basale cell at higher magnification showing desmosomes (D) and the basement membrane.  $\times 2550$ ; (bar  $1 \mu\text{m}$ ).

cytoplasm of these cells was similar to those of the stratum basale; however, the tonofilaments were predominantly present. The adjacent cells showed interdigitating villi-like projections of variable shapes and sizes (Figure 22).



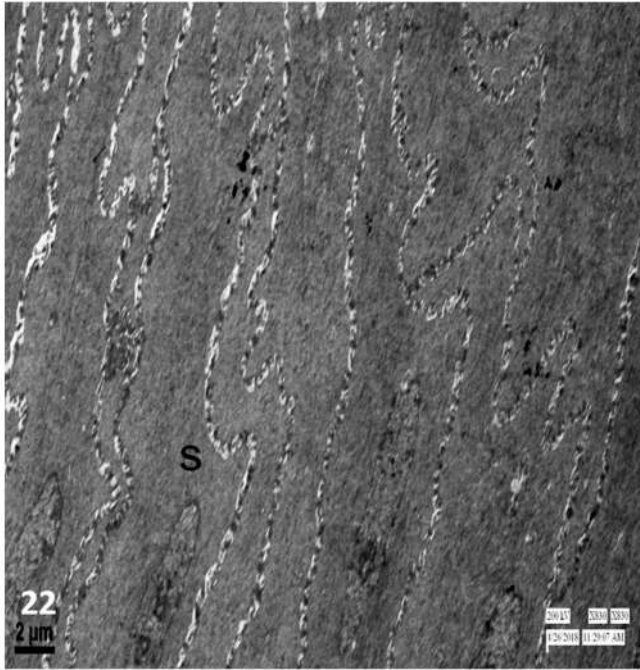


**Figure 22:** Transmission electron micrograph of the paraepiglottic tonsil of buffalo showing stratum spinosum (S) of stratified squamous keratinised epithelium.  $\times 830$ ; (bar 2  $\mu\text{m}$ ).

The nuclei of the stratum granulosum showed their longitudinal axis parallel to the length of the epithelium. Moreover, such nuclei showed condensation of chromatin irregularly throughout the nucleoplasm

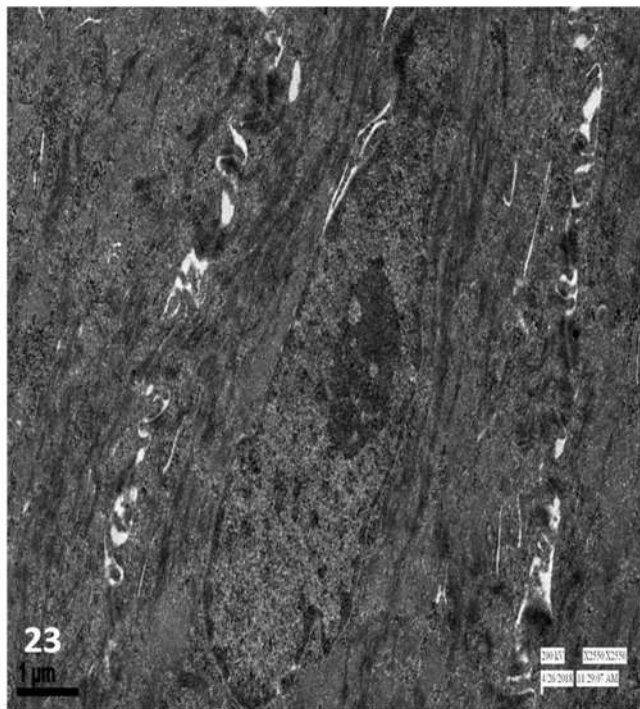


**Figure 23:** Transmission electron micrograph of the paraepiglottic tonsil of buffalo showing stratum granulosum cells.  $\times 2550$ ; (bar 1  $\mu\text{m}$ ).

except for smaller clumps localised towards the outer nuclear membrane (Figure 23). The nucleoli were distinct in some of the cells only. The outer surface of these nuclei was irregular, and some of these presented indentations. The cytoplasm of these cells showed a lesser concentration of the cell organelles, including the filaments. Their intercellular spaces presented interdigitating villi similar to those of other strata. The electron-dense nuclei of the stratum corneum were visible only in a few cells with pyknotic and degenerative changes (Figure 24).

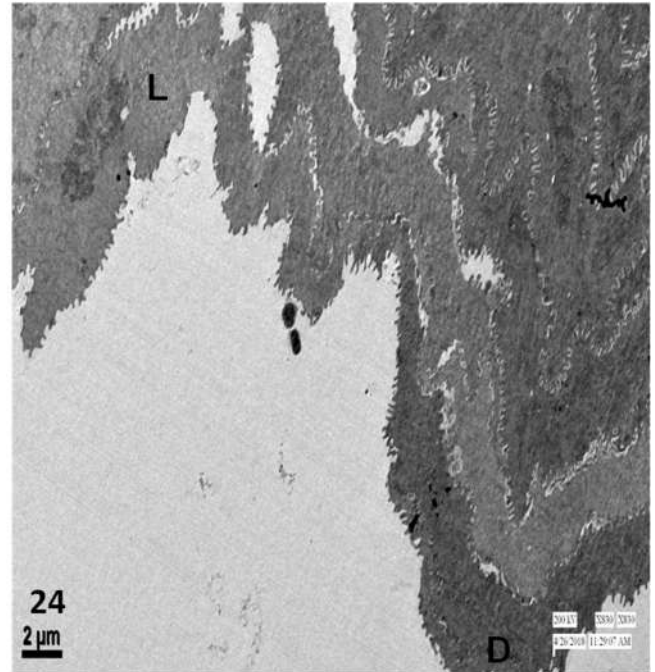


**Figure 24:** Transmission electron micrograph of the paraepiglottic tonsil of buffalo showing light (L) and dark (D) cells of stratum corneum of keratinised epithelium.  $\times 830$ ; (bar 2  $\mu\text{m}$ ).

The stratified squamous non-keratinised epithelium shared the ultrastructural features similar to those of the keratinised epithelium except the more superficial cell layers toward the free surface with small microvilli giving a spiky appearance (Figure 25). The nuclei were distinguished only in some of the cells in this layer, and they had chromatin being condensed into smaller clumps towards the outer nuclear membrane. The interdigitating villi-like projections were fewer than those of other strata.

The stratum basale cells of reticular epithelium were low cuboidal, and their nuclei were horizontally placed rather than vertically oriented (Figure 26). There was comparatively more infiltration of the lymphoid cells in between the epithelial cells. The other features of the epithelial cells were similar to those in the region of the

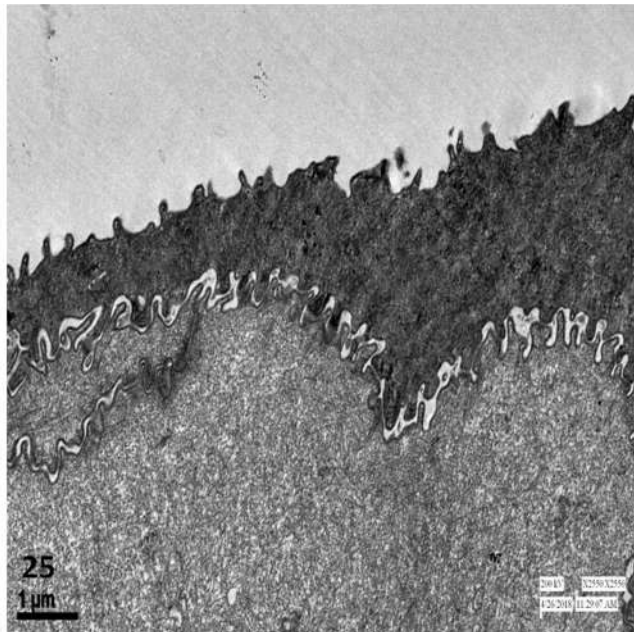


**Figure 25:** Transmission electron micrograph of the paraepiglottic tonsil of buffalo showing the pricky appearance of the free surface of the non-keratinised epithelium.  $\times 2550$ ; (bar 1  $\mu\text{m}$ ).

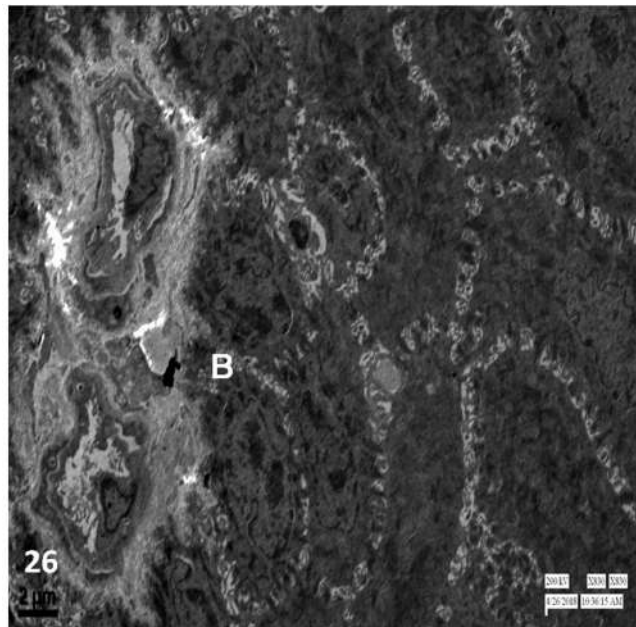


**Figure 26:** Transmission electron micrograph showing low cuboidal cells of stratum basale (B) of the reticular epithelium.  $\times 830$ ; (bar 2  $\mu\text{m}$ ).

non-keratinised epithelium. The superficial cells were of different shapes and sizes. At places, the low cuboidal cells having electron-lucent nuclei with one centric/eccentric nucleolus were observed. The cytoplasm of these cells presented few cell organelles and few vacuolated structures; however, the concentration of the mitochondria, endoplasmic

reticulum and Golgi apparatus was comparatively increased. The free surface of these cells showed small microvilli-like projections (Figure 27). The propria-submucosa showed fine blood capillaries, lymphoid cells, particularly lymphocytes, few plasma cells, and macrophages. In addition, a few high endothelial venules (HEV's) were also observed.

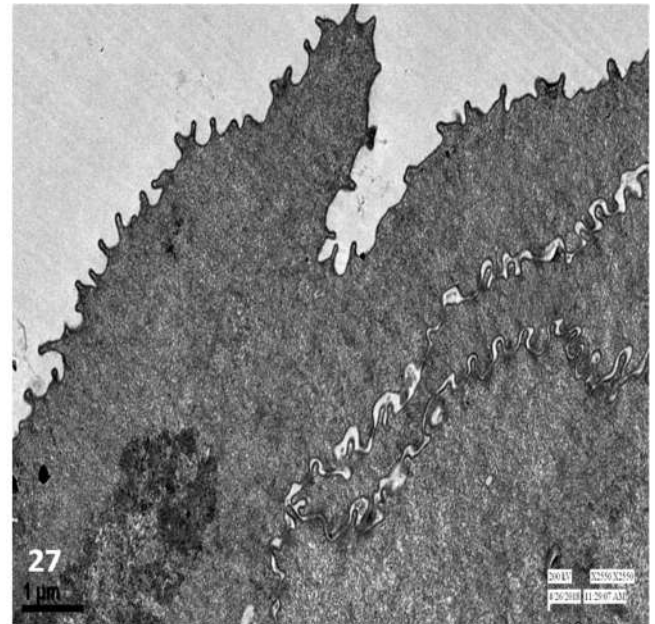


**Figure 27:** Transmission electron micrograph at higher magnification showing microvilli-like projections on the free surface of the reticular epithelium.  $\times 2550$ ; (bar 1  $\mu\text{m}$ ).

## DISCUSSION

The epithelial lining of the paraepiglottic tonsil towards the outer surface was stratified squamous keratinised to non-keratinised type as reported in the sheep [18, 23], pig [19, 24] and camel [1, 25, 26]. The stratified squamous keratinised epithelium was comprised of a varying number of rows in strata spinosum, granulosum and corneum as reported in the sheep except for stratum basale [18]. The basal surface of the epithelium showed the presence of interpapillary pegs of irregular shape, whereas the free surface presented an undulating surface as observed in the sheep [18]. Similarly, the non-keratinised epithelium presented a varying number of rows in strata spinosum and superficiae as reported in the sheep [18] and the pig [19]. Its free surface was slightly uneven whereas, and the basal surface was almost uniform, having small interpapillary pegs. The stratum basale had a single row of high cuboidal or low columnar cells, with a round to oval elongated basophilic nuclei, with their longitudinal axis perpendicular to the basement membrane as reported

in the pig [19]. The stratum spinosum had a varying number of cell layers, which in the pig [19] constituted 4-8 rows of cells. The cells of the stratum superficiale were also varying in number and rows at different levels of extents of the epithelium. In the pig, about 10-12 of such rows were reported [22]. The nuclei of the deeper layer were round to oval, having a vacuolated appearance, whereas nuclei of more superficially placed cells were basophilic and presented degenerative changes as observed in the sheep [18] and pig [19].

The reticular epithelium was a modification of stratified squamous non-keratinised epithelium due to infiltration of underlying lymphoid tissue as reported in sheep [18] and pigs [19]. Such epithelial structural modifications have been described in the human palatine tonsil [27] and the tonsils of buffalo [10, 17, 23]. At places, the lymphoid tissue was so predominant that it led to the interrupted basement membrane, and it was difficult to discern the epithelial cells and different strata. The reticular epithelium also presented a spongy appearance towards depressions or shallow crypts. The dominance of non-epithelial cells resulted in the loss of classical epithelial characteristics and the appearance of the functional lymphoid compartment, which still maintained its protective function [28, 29]. Direct transepithelial access of antigen may result in greater influx and recruitment of non-epithelial cells in a particular patch, but the appropriate balance of epithelial and non-epithelial cells is required to preserve efficient mucosal protection as locally produced IgA is not recycled but continually synthesised by the epithelial cells [28]. B and T cells infiltrated the whole epithelial thickness [27], whereas plasma cells located within this epithelium in a patchy distribution [28]. Hence, the favourable environment and subsequent interaction between various immune cells in the reticular epithelium may likely contribute to the first line of defence [27].

The histoarchitecture of the propria-submucosa was similar to findings observed in the sheep [18] and the pig [19]. The distribution of the lymphoid tissue observed in the present study was in harmony with findings reported in the sheep [18, 23], pig [19], and camel [26]. The lymphoid follicles were stacked one upon another, oriented perpendicular to the length of the epithelium. The number of these follicles varied from 15-23 in the pig [19], whereas, in ovine, the diffused aggregations of lymphoid tissue were designated tonsillar nodule [30] because of the absence of epithelial crypts. The lightly stained

germinal center and darkly stained corona towards the periphery of the lymphoid follicles was similar to findings in the pig [19]. The morphology of these follicles can be influenced by antigenic stimulation as a prerequisite to induce germinal centers [31]. The follicles of the buffaloes were comprised of lymphocytes of different sizes, a few plasma cells, and macrophages, and these were quantified mainly as CD21+ and CD3+ lymphocytes in the ovine [32]. High endothelial venules, fine blood capillaries, macrophages, and plasma cells were observed as reported in the sheep and pig [18, 19]. The HEVs were involved in the trafficking of T and B lymphocytes from blood to tonsil and back to the circulation via lymph [33], and migration of these lymphoid cells is strictly regulated by the expression of multiple adhesion molecules and receptors for chemo-attractant (chemokine receptors) that interact with corresponding ligands on endothelial and stromal cells [34]. The lymphocytes enter immunological effector sites by diapedesis through high endothelial venules (HEVs) [4]. Thus, lymph vessels and HEV's served as the structural basis of the common mucosal immune system by providing a route for lymphocytes recirculation [35, 36]. The periphery of these lymphoid aggregations in the present study was surrounded by a comparatively denser arrangement of collagen fibres, along with fine meshwork of reticular fibers as observed in the sheep [18]. The sero-mucous glandular acini, with a predominance of later, were present in clusters below the lymphoid tissue. The mucous glandular acini showed a strong PAS-positive reaction for glycogen, weakly sulfated acidic mucosubstances, hyaluronic acid, sialomucins, and mucins, as reported in the sheep [18] and the pig [19]. The mucous acini showed a predominance of acidic mucopolysaccharides as reported in the sheep [18], contrary to the neutral mucopolysaccharides in the pig [19]. A strongly positive reaction for acidic mucopolysaccharides was also exhibited by colloidal iron as reported in the pig [18]. A strong reaction for performic acid-Alcian blue in the mucous acini indicated the presence of more than 4% cysteine. The ducts did not exhibit any PAS-positive reaction.

SEM of the mucosal surface of the paraepiglottic tonsils demonstrated undulating appearance with crest and folds as reported in pig [19]. The majority of the surface was uniform; however, one to four round or oval tonsillar nodules protruded into the pharyngeal lumen covered by a non-keratinised stratified squamous epithelium in the ovine [37]. The squamous cells lining the surface were continuous with each other

as reported in pig [19], tonsil of the soft palate and lingual tonsil of buffaloes [8, 14]. Higher magnification of these cells showed varying patterns and arrangements of the microplacae as described in sheep [37], buffalo [14] and pig [19]. Small holes observed on the surface were openings of the glandular ducts as observed in horses [2] and buffalo [14]. A whorl-like arrangement of the cells lined the surface of the lumen, having a microvillus-like arrangement with the absence of the microplacae as reported in the lingual tonsil of buffaloes [14].

TEM of the stratified squamous keratinised epithelium of the paraepiglottic tonsils shared many ultrastructural features with those previously described in the lingual tonsil [14]. The stratum basale had electron-dense vertical oriented nuclei with small clumps of chromatin material as observed in the tonsil of the soft palate [8] and lingual tonsil [14] of buffaloes. The nuclei in the stratum spinosum were electron-lucent, and the outer surface of the nuclei in both the strata presented nuclear indentations as observed in the lingual tonsil [14]. The cytoplasm of the cells of stratum granulosum showed a lesser concentration of the cell organelles and few filaments as observed in the lingual tonsil [14]. The stratum corneum had very electron-dense nuclei visible only in a few cells, and these were showing degenerative changes as observed in horses [2] and buffalo [14]. The stratified squamous non-keratinised epithelium shared similar ultrastructural features to those of the keratinised epithelium except the more superficially placed cell layers towards the free surface presented small microvilli giving the spiky appearance as described in the lingual tonsil of the horse and buffalo [2, 14], tonsil of the soft palate [8] and human palatine tonsil [28]. The epithelium consisted of more than 10 layers of squamous cells, and the reticular epithelium was related to lymphoid nodules in the ovine [18]. The stratum basale of the reticular epithelium comprised of low cuboidal cells having horizontally placed nuclei showed more infiltration of the underlying lymphoid cells as reported in the ovine [37]. The other features of the epithelial cells were similar to those in the region of the non-keratinised epithelium. The propria-submucosa showed fine blood capillaries, lymphoid cells, particularly lymphocytes, few plasma cells and macrophages as observed in the tonsil of the soft palate [8]. Few HEV's were also observed, which presented features similar to those seen in the tonsils of horses [38], buffalo [14], camel [39], ovine [37] and porcine [24].

The small-sized paraepiglottic tonsil, in comparison to other tonsils, has qualitatively lesser reticular epithelium, lymphoid tissue and follicles with different cell types, HEVs and different types of mucopolysaccharides, but their presence makes it an immunological organ that might have significance in local defence mechanism.

## CONCLUSION

The modification of stratified squamous non-keratinised epithelium into the reticular epithelium might play an important role due to its close association with the underlying lymphoid tissue, especially the lymphoid follicles. The presence of glycogen and other mucopolysaccharides in the secretions of mucous glands might have a role in the entrapment of foreign antigens. The mucosal surface under SEM revealed squamous cells consisting of varying patterns of microplacae. The study also demonstrated cellular details of the different strata of different types of epithelia, including the reticular epithelium. The paraepiglottic tonsils shared some structural features similar to those of lingual tonsils and tonsil of the soft palate of buffaloes. The presence of lymphoid and plasma cells along with high endothelial venules through lesser than other tonsils is suggestive that the paraepiglottic tonsils might have a localised immunological role.

## ACKNOWLEDGEMENT

The first author was granted a fellowship sponsored by the Indian Council for Cultural Relation ICCR (Africa scholarship section) for his PhD programme. The authors gratefully acknowledge the EM Lab., AIIMS, New Delhi, India, for providing the electron microscopy facility.

## CONFLICT OF INTEREST

The authors do not have any conflict of interest.

## FUNDING STATEMENT

The authors did not get any funding for this research work except fellowship to the first author for his Doctoral programme.

## REFERENCES

- [1] Achaaban MR, Mouloud M, Tligui NS, El Allali K. Main anatomical and histological features of the tonsils in the camel (*Camelus dromedarius*). *Trop Anim Health Prod* 2016; 48: 1653-1659. <https://doi.org/10.1007/s11250-016-1139-x>

- [2] Kumar P, Timoney JF. Histology and ultrastructure of the equine lingual tonsil. II. Lymphoid tissue and associated high endothelial venules. *Anat Histol Embryol* 2005; 34: 98-104. <https://doi.org/10.1111/j.1439-0264.2004.00579.x>
- [3] Horter DC, Yoon JK, Zimmerman JJ. A review of porcine tonsils in immunity and disease. *Anim Health Res Rev* 2003; 4: 143-155. <https://doi.org/10.1079/AHRR200358>
- [4] Brandtzaeg P, Pabst P. Let's go mucosal: communication on slippery ground. *Trends Immunol* 2004; 25: 570-578. <https://doi.org/10.1016/j.it.2004.09.005>
- [5] Bernstein JM, Bækkevold ES, Brandtzaeg P. Immunobiology of the tonsils and adenoids. In: Mestecky J, Lamm ME, Strober W. *Mucosal Immunology*. 3rd ed. San Diego: Elsevier, Academic Press; 2005. <https://doi.org/10.1016/B978-012491543-5/50094-2>
- [6] Liebler-Terino EM, Pabst R. MALT structure and function in farm animals. *Vet Res* 2006; 37: 257-280. <https://doi.org/10.1051/vetres:2006001>
- [7] Girgiri IA, Kumar P. Histology, histochemistry and scanning electron microscopy of tonsil of the soft palate of buffalo (*Bubalus bubalis*). *Indian J Vet Anat* 2018; 30: 58-63.
- [8] Girgiri IA, Kumar P. Transmission electron microscopy of tonsil of the soft palate of buffalo (*Bubalus bubalis*). *Haryana Vet* 2018; 57: 59-61.
- [9] Zidan M, Pabst R. The microanatomy of the palatine tonsils of the buffalo (*Bos Bubalus*). *Vet. Immunol Immunopathol* 2011; 139: 83-89. <https://doi.org/10.1016/j.vetimm.2010.08.006>
- [10] Girgiri IA, Kumar P. Light microscopic studies on the palatine tonsil of the buffalo (*Bubalus bubalis*). *Vet Res Int* 2018; 6: 60-66. <https://doi.org/10.6000/1927-520X.2021.10.02>
- [11] Girgiri IA, Kumar P. Histology, histochemistry and ultrastructure of the nasopharyngeal tonsil of buffalo (*Bubalus bubalis*). *Anat Histol Embryol* 2019; 48: 375-383. <https://doi.org/10.1111/ah.e.12452>
- [12] Ez Elarab SM, Zidan M, Zaghloul MD, Derbalah AE. Histological structure of the lingual tonsils of the buffalo calf (*Bos Bubalus*). *Alexandria J Vet Sci* 2016; 49: 78-84. <https://doi.org/10.5455/ajvs.222704>
- [13] Girgiri IA, Kumar P. Histological and histochemical studies on the lingual tonsil of the buffalo (*Bubalus bubalis*). *J Buffalo Sci* 2019; 8: 68-76. <https://doi.org/10.6000/1927-520X.2019.08.03.3>
- [14] Girgiri IA, Kumar P. Scanning and transmission electron-microscopic studies on the lingual tonsil of the buffalo (*Bubalus bubalis*). *J Buffalo Sci* 2020; 9: 5-12. <https://doi.org/10.6000/1927-520X.2020.09.02>
- [15] Girgiri IA, Kumar P. Light and electron-microscopic studies on the tubal tonsil of the buffalo (*Bubalus bubalis*). *J Buffalo Sci* 2020; 9: 60-70. <https://doi.org/10.6000/1927-520X.2020.09.08>
- [16] Casteleyn C, Breugelmans S, Simoens P, Van den Broeck W. The tonsil revisited: Review of the anatomical localisation and histological characteristics of the tonsils of domestic and laboratory animals. *Clin Dev Immunol* 2011; 21: 1-14. <https://doi.org/10.1155/2011/472460>
- [17] Casteleyn C, Simoens P, Cornillie P, Van den Broeck W. Larynx associated lymphoid tissue in young cattle (LALT). *Vet Immunol Immunopathol* 2008; 124: 394-397. <https://doi.org/10.1016/j.vetimm.2008.04.008>
- [18] Kumar P, Singh G, Nagpal SK. Histological studies on the paraepiglottic tonsil of the sheep. *Indian J Anim Sci* 2010; 80: 650-652.
- [19] Ranjit, Kumar P, Kumar P, Singh G. Histology, histochemistry and scanning electron microscopy of paraepiglottic tonsil of the young pigs. *Indian J Vet Anat* 2015; 27: 30-33.
- [20] Luna LG. *Manual of histologic staining methods of Armed Forces Institute of Pathology*. 3rd ed. New York: McGraw-Hill Book Company; 1968.
- [21] Crossman GA. A modification of Mallory's connective tissue stain with a discussion of principles involved. *Anat Rec* 1937; 69: 33-38. <https://doi.org/10.1002/ar.1090690105>
- [22] Pearse AGE. *Histochemistry: theoretical and applied*. 3rd ed. London: Churchill Livingstone; 1968.
- [23] Casteleyn C, Van den Broeck W, Simoens P. Histological characteristics and stereological volume assessment of the ovine tonsils. *Vet Immunol Immunopathol* 2007; 120: 124-135. <https://doi.org/10.1016/j.vetimm.2007.07.010>
- [24] Liu Z, Yu Q, Li, P, Yang Q. Histological and ultrastructural examinations of porcine tonsils. *Anat Rec* 2012; 295: 686-690. <https://doi.org/10.1002/ar.21534>
- [25] Yang C, Zang C, Bai Z, Yuan G, Shoa B, Zhao S, Wang J. Anatomical localisation and histology of larynx-associated lymphoid tissue (LALT) in the adult Bactrian camel (*Camelus bactrianus*). *J Camel Prac Res* 2010; 17: 99-102.
- [26] Yang C, Yuan G, Xu Z, Shoa B, Wang J. The topography and the microscopic structure of tonsils in the adult Bactrian camel (*Camelus bactrianus*). *J Camel Prac Res* 2011; 18: 155-163.
- [27] Brandtzaeg P. Immunobiology of the tonsils and adenoids. *Mucosal Immunol* 2015; 2: 1985-2016. <https://doi.org/10.1016/B978-0-12-415847-4.00103-8>
- [28] Perry ME. The specialised structure of crypt epithelium in the human palatine tonsil and its functional significance. *J Anat* 1994; 185: 111-127.
- [29] Brandtzaeg P. Immunopathological alterations in tonsillar disease. *Acta Otolaryngol Suppl (Stockh)* 1988; 454: 64-69. <https://doi.org/10.3109/00016488809125007>
- [30] Cocquyt G, Baten T, Simoens P, Van den Broeck W. Anatomical localisation and histology of ovine tonsils. *Vet Immunol Immunopathol* 2005; 107: 79-86. <https://doi.org/10.1016/j.vetimm.2005.03.012>
- [31] Monteleone G, Peluso I, Fina D, Caruso R, Andrei F, Tosti C. Bacteria and mucosal immunity. *Dig Liver Dis* 2006; 38: 256-260. [https://doi.org/10.1016/S1590-8658\(07\)60005-X](https://doi.org/10.1016/S1590-8658(07)60005-X)
- [32] Breugelmans S, Van den Broeck W, Demeyere K, Meyer E, Simoens P. Immunoassay of lymphocyte subsets in ovine palatine tonsils. *Acta Histochem* 2011; 113: 416-422. <https://doi.org/10.1016/j.acthis.2010.03.001>
- [33] Schaer P, Willmann K, Lang AB, Lipp M, Loetscher P, Moser B. CXC chemokine receptor 5 expression defines follicular homing T cells with B cell helper function. *J Exp Med* 2000; 192: 1553-1562. <https://doi.org/10.1084/jem.192.11.1553>
- [34] Kunkel EJ, Butcher EC. Chemokines and the tissue-specific migration of lymphocytes. *Immunity* 2002; 16: 1-4. [https://doi.org/10.1016/S1074-7613\(01\)00261-8](https://doi.org/10.1016/S1074-7613(01)00261-8)
- [35] Kumar P, Kumar P, Kumar S. Light and scanning electron microscopic studies on the nasopharyngeal tonsil of the goat. *Indian J Anim Sci* 2006; 76: 452-455.
- [36] Belz GT. An unusual structure of venules in the tonsils of the soft palate of young pigs. *J Anat* 1998; 192: 131-135. <https://doi.org/10.1046/j.1469-7580.1998.19210131.x>
- [37] Casteleyn C, Cornelissen M, Simoens P, Van den Broeck W. Ultramicroscopic examination of the ovine tonsillar epithelia. *Anat Rec* 2010; 293: 879-889. <https://doi.org/10.1002/ar.21098>

[38] Kumar P, Timoney JF. Immunohistochemistry and ultrastructure of the equine palatine tonsil. *Anat Histol Embryol* 2005; 34: 192-198.  
<https://doi.org/10.1111/j.1439-0264.2005.00594.x>

[39] Zidan M, Pabst R. The microanatomy of the palatine tonsils of the one-humped camel (*Camelus dromedarius*). *Anat Rec* 2009; 292: 1129-1197.  
<https://doi.org/10.1002/ar.20948>

---

Received on 26-05-2021

Accepted on 18-10-2021

Published on 27-10-2021

<https://doi.org/10.6000/1927-520X.2021.10.13>

© 2021 Girgiri and Kumar; Licensee Lifescience Global.

This is an open access article licensed under the terms of the Creative Commons Attribution License (<http://creativecommons.org/licenses/by/4.0/>) which permits unrestricted use, distribution and reproduction in any medium, provided the work is properly cited.